forum acusticum 2026
8-12 September · Graz, Austria

THE INFLUENCE OF CEILING SHAPE ON SPATIO-TEMPORAL SOUND ENERGY INCIDENCES IN CONCERT HALLS

Linus Staubach[1, 2], Eckard Mommertz[2], Stefan Weinzierl[1]

[1] *Audio Communication Group, TU Berlin: Technische Universität Berlin, Germany*
[2] *Müller-BBM Building Solutions GmbH, Helmut-A.-Müller-Straße 1 – 5, 82152 Planegg, Germany*

Abstract

The architectural and acoustic designs of concert halls influence their overall appearance and aesthetic appeal. However, it can be challenging to achieve both visual appeal and acoustic excellence. Concert halls are often categorized as vineyard or shoebox types, which are specified by the relationship between the orchestra and the audience, the surrounding surfaces, and the general shape of the space. In contrast, ceiling shapes can vary independently of typology and range from horizontal to curved to tilted.

This paper examines how ceiling geometry affects the spatial and temporal distribution of sound energy to listeners in concert halls. A parametric study is presented in which the shape, height, and surface properties of the ceiling are varied using the ray tracing tool misuka, which was developed at TU Berlin. Substantial differences in sound energy decay were found when comparing non-flat (e.g., pyramidal) and flat ceilings, depending on their surface structure. Conversely, only minor changes were observed in established sound strength parameters. Furthermore, changes in spatio-temporal sound energy incidence are discussed.

Keywords: *room acoustics, concert halls*

1. Acoustic-architectural interplay

During the planning phase of a concert hall, several decisions in terms of acoustical and visual aesthetics have to be made. However, excellent properties are expected from both. From an acoustical point of view, the influences of architectural decisions on the acoustical properties of the hall have to be understood and matched with the desired expectations. Simultaneously, findings from the perception of sound can lead to different architectural approaches. The latter can be seen by looking at a historical overview of different basic shapes of concert halls.

Until the middle of the 20$^{\text{th}}$ century, the predominant shape for a concert hall was rectangular, also denoted as *shoebox*. Until now, its general acoustical properties have been rated as highly preferable [1]. With the construction of the Philharmonie Berlin in 1963, the *vineyard* or *surround*-shape halls mark a rather radical but successful change in approaching architecture and acoustics. Characteristic for this typology is the more central position of the orchestra. The audience is located on terraces all around, providing excellent sightlines and therefore a good supply with direct sound. Special attention was paid to surfaces that provide listeners with early reflected sound energy from all around, which is supposed to acoustically surround the audience [1]. A prime example of a reflection-focused design of a concert hall is the Christchurch Town Hall. Large tilted reflectors surrounding the listeners in the upper wall area provide plenty of lateral sound components. This is supposed to increase spatial impression (SI) and thus give a certain "premium quality of sound" [2]. Because early energy is directed towards a highly absorbing surface, namely the audience, this design can be deficital in preserving sound energy and thus providing late reverberance.

Independent on its general typology, the ceiling, including the upper wall structure of concert halls, can be found of various shapes. Although the most common one for shoebox halls is a flat horizontal ceiling, the Tokyo Opera City Concert Hall (TOC) marks an exception with its pyramid-shaped ceiling with a stepped surface structure [3]. Equal variety can be seen in vineyard-type halls, where shapes range from almost horizontal (e.g., in the Gewandhaus, Leipzig) via curved to tilted ones (e.g., Philharmonie, Berlin; Elbphilharmonie, Hamburg). In most cases, the ceiling shape is a combination of larger surfaces with smaller irregularities and elements. Although concert hall typologies have been part of extensive previous

Corresponding author: *Linus.Staubach@mbbm-bso.com.*

research regarding perceptual and physical properties, the influence of the ceiling structure remains mostly unconsidered.

2. Parametric simulation study

A parametric study based on room acoustical simulations has been carried out to inspect changes in sound incidences in the audience caused by variations in ceiling shapes. In the simulations, the total height of the ceiling geometry has been incrementally varied from a flat ceiling to four abstracted ceiling shapes shown in Fig. 1.

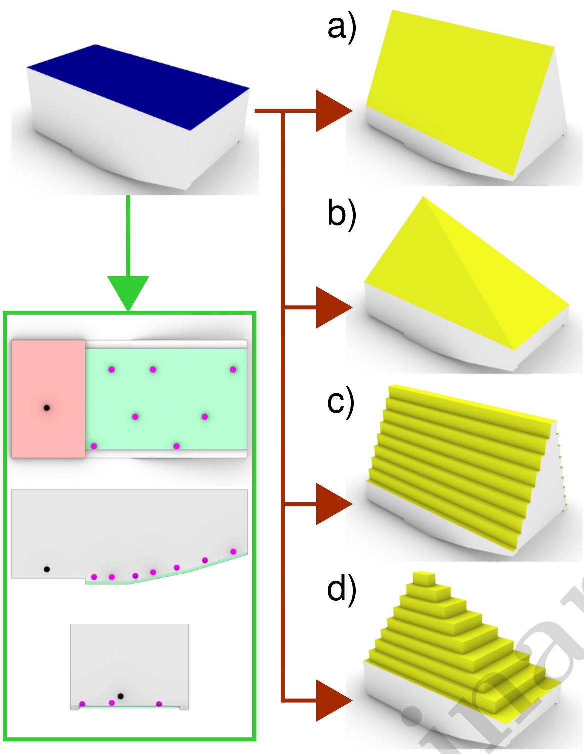

Figure 1: Simulated base concert hall model with ground plan and sectional views (see green box) with audience surfaces marked in green, stage surface in red and hall surfaces in white. Dots in the stage and audience area mark the source and receiver positions. Modified ceiling shapes derived from the initial, blue coloured flat or horizontal ceiling are illustrated on the right hand side, where maximum states are coloured in yellow. The shapes are refered to as gable (a)), pyramid (b)), stepped gable (c)) and stepped pyramid (d)).

The calculations have been performed with *misuka* [4], an open-source acoustical ray tracing algorithm. A suitable version of the tool had to be built to be used as a Python package. In addition, Python scripts for the simulations were developed that implement the general acoustic simulation conditions, the geometry modifications of the ceilings, and the room acoustical parameters. To verify the plausibility of the results, a comparison with the commercial simulation tool *Odeon* has been made.

2.1. Concert hall models and ceiling shapes

The starting point for each series of simulations is a shoebox-shaped hall with a raked seating area. With overall dimensions of $20\,\mathrm{m} \times 40\,\mathrm{m} \times 16\,\mathrm{m}$ $(w \times l \times h)$ and a volume of $V = 11416\,\mathrm{m}^2$, it can be seen as a small concert hall for symphonic music. The estimated seating capacity is about 1000 listeners, resulting in a volume per listener ratio of $\frac{V}{N} = 11.4\,\mathrm{m}^3$.

Based on current ceiling designs in concert halls, two simplified types, flat and raked or pointed ceilings, will be considered. Examples of these shapes include the Musikvereinssaal in Vienna or the Konzerthaus in Berlin, with their flat ceilings, as well as the Philharmonie in Berlin or the TOC, with their pointed or raked ceilings [1]. The series of simulations iterates between both types starting from the flat ceiling and ending in two abstract geometries, shaped like a gable roof and an asymmetric pyramid. Furthermore, different structures of ceiling surfaces are considered as stepped variants, inspired by the ceiling of the TOC [3]. The minimum and maximum states of the simulated ceiling geometries are presented in Fig. 1.

Variations in ceiling shape are implemented by varying the total height of the ceiling structure. The corresponding vertices are shifted vertically to preserve the horizontal dimensions. Simultaneously, the ceiling structure is lowered to ensure equal volume across all variations. In their maximum states, the ceiling geometries account for 77% (gable-like variants) and 68% (pyramid-like shapes) of the total room height. Changes in total surface area are inevitable, whereby deviations in absorption area and room acoustical parameters are to be expected.

2.2. Simulation conditions

The acoustical surface properties of the concert hall models are specified in Table 1, resulting in a Sabine reverberation time of $T_{\mathrm{Sabine,flat}} = 2.1\,\mathrm{s}$ and a simulated one of $T_{\mathrm{flat}} = 2\,\mathrm{s}$ (see Fig. 2) for the initial hall model with a flat ceiling.

Table 1: Absorption and scattering coefficients assigned to the surfaces of the simulated concert halls.

Surface name	absorption coefficient α	scattering coefficient δ
audience	0.86	0.7
stage	0.62	0.4
ceiling	0.09	0.3
hall surfaces	0.09	0.3

The simulations have been performed at a single frequency of 1000 Hz, and thus frequency dependencies of parameters and surface properties are neglected. Air damping was considered according to ISO 9613-1 [5] with a relative humidity of $h_{\mathrm{r}} = 50.0\%$, an atmospheric pressure of $p_{\mathrm{a}} = 101.4\,\mathrm{kPa}$ and a temperature of $\vartheta = 20.0\,^{\circ}\mathrm{C}$. The speed of sound is considered with $c = 343\,\frac{\mathrm{m}}{\mathrm{s}}$.

The results from the misuka simulations represent impulse responses in the form of energy time curves $H(t)$, extracted in the first order Ambisonics format (FOA), thus including one omnidirectional and three directional channels. The energies are gathered in a time resolution of 1/48000 s. For each combination of the one source and seven receiver positions (see Fig. 1), a total number of $n_{\mathrm{r}} = 1062961$ rays has been calculated. Across all calculations, the spatial distribution of the rays has been kept constant to preserve comparability between the results.

2.3. Room acoustical parameters

From the energy time curves $H(t)$, which are equivalent to squared impulse responses $p^2(t)$, several room acoustical parameters are calculated to quantify the effects of the ceiling shapes. They are chosen to retrieve information about sound energy contributions in respect of temporal and spatial aspects and the slope of sound energy decay, thus the reverberation.

2.3.1. Reverberation

The physical and perceptual reverberation properties of a room are described by the reverberation time T and the early decay time EDT [6].

T is defined as the time it takes the sound energy to decay 60 dB from an acoustically excited room in a steady state. It can be estimated from the decay of the recorded sound pressure level or the level of the energy decay curve (EDC), the backward-integrated impulse response. A linear regression is performed in an interval starting from 5 dB below the direct sound and ending above static noise, or in this case uncertainties due to simulation limits. Here, an estimation interval of 20 dB has been chosen. Subsequently, the decay time in this interval is extrapolated to a decay of 60 dB, while the reverberation time is denoted as T_{20}.

The EDT is calculated to provide a parameter closer to the perception of reverberation compared to T. Its estimation procedure is nearly equivalent to that of T, but the regression interval spans the first 10 dB of the decay of the sound energy.

2.3.2. Sound energy relations

The loudness of a concert hall is estimated by the sound strength G. It is defined by

$$G = 10 \cdot \lg \frac{\int_{t_1=0}^{t_2=\infty} H(t)\mathrm{d}t}{\int_0^\infty H_{10}(t)\mathrm{d}t}\,\mathrm{dB}, \qquad (1)$$

where $H(t)$ denotes the energy time curve measured with an omnidirectional source and receiver at distinct points in a concert hall. $H_{10}(t)$ describes the energy time curve measured with an equivalent source and receiver combination in a distance of 10 m under free-field conditions. The integration intervals span from the start of the impulse response $t_1 = 0\,\mathrm{s}$, thus the direct sound, to its end $t_2 = \infty\,\mathrm{s}$.

Total sound energy contributions to the sound strength can be divided into an early part consisting of the direct sound and the early reflections and a late part, denoting energies from the statistical decay. The transition time between both parts is defined to be at 80 ms. From this, the early sound strength G_{early} can be derived from Eq. (1) by changing the upper integration limit of $H(t)$ to $t_2 = 80\,\mathrm{ms}$. Similarly, G_{late} can be derived from Eq. (1) by substituting the lower integration limit of $H(t)$ with $t_1 = 80\,\mathrm{ms}$.

By further parameterizing these transition limits with the variable τ, functions representing the relative buildup of sound energy $G_{\mathrm{early}}(\tau)$ and relative decay of sound energy $G_{\mathrm{late}}(\tau)$ can be derived. The range of τ is equal to the length of the impulse response starting from direct sound. Additionally, $G_{\mathrm{late}}(\tau)$ can be seen as the EDC normalised to the reference sound level $L_{\mathrm{p},10}$, the total level of $H_{10}(t)$. It is thereby defined as

$$\begin{aligned} G_{late}(\tau) &= 10 \cdot \lg \frac{\int_{t_1=\tau}^{t_2=\infty} H(t)\mathrm{d}t}{\int_0^\infty H_{10}(t)\mathrm{d}t}\,\mathrm{dB} \\ &= EDC(t=\tau) - L_{\mathrm{p},10}\,\mathrm{dB}. \end{aligned} \qquad (2)$$

2.3.3. Spatial parameters

The spatial perception of sound in concert halls can be estimated using parameters based on directional receivers according to ISO 3382-1 [6]. The early lateral energy fraction J_{LF} is an estimator of the apparent source width (ASW). It is calculated from the first 80 ms of an impulse response as the relation between the energy measured with a figure-of-eight receiver and an omnidirectional one. The null of the directional receiver is oriented towards the source.

The impression of listener envelopment (LEV) can be estimated by the relative late lateral energy level L_{J}, sometimes denoted as G_{LL} or $G_{\mathrm{lateral,late}}$, which inspects the lateral contributions after 80 ms. It is calculated similarly to G_{late} described in Section 2.3.2, where the omnidirectional receiver $H(t)$ is substituted with a figure-of-eight receiver $H_{\mathrm{L}}(t)$ as used in J_{LF}.

Furthermore, the perceptual time periods representing ASW, LEV and *running reverberation* proposed by Green et al. [7] are calculated as variants of L_{J}. The lateral figure-of-eight receiver approximates the directional dependence in the time periods. Further directional information is gained by a vertically oriented variant and another one directed towards the front and back.

3. Simulation results

The results of the room acoustical simulations are shown for four representative ceiling shapes, as presented in Fig. 1. The ceiling height is normalised as *ceiling geometry deformation*, where 0 represents a flat horizontal ceiling and 1 the maximum state of the altered ceiling shape. All results represent averaged values across all receiver positions.

The series of simulations has been repeated with three additional source positions, an altered pyramid ceiling shape, and a more freeform-shaped hall with a pyramid-shaped ceiling geometry. The resulting effects remain equal compared to the findings presented below.

3.1. Reverberation

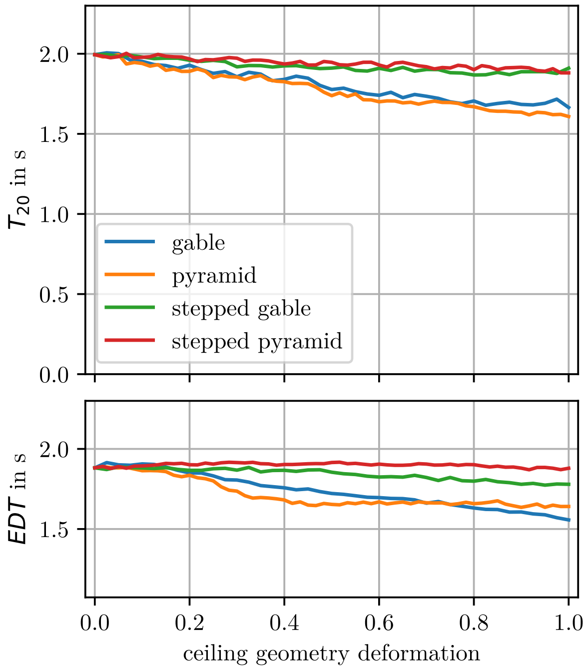

Figure 2: Reverberation times T_{20} as well as the early decay times EDT during the incremental deformation of four ceiling geometries from flat or horizontal to their maximum ceiling shape.

Changes in reverberation times T_{20} and early decay times EDT as a function of ceiling geometry deformation are presented in Fig. 2.

The simulation results show that T_{20} as well as the EDT are reduced when changing the height of the ceiling geometry. Unstructured ceiling surfaces (*gable* and *pyramid*) lead to a reduction mostly proportional to the ceiling geometry height. The change in T_{20} is approximately -19%, when comparing the maximum ceiling deformation state with the flat ceiling state, where $T_{20,\text{flat}} = 2\,\text{s}$. Stepped ceilings (*stepped gable* and *stepped pyramid*) mitigate the effect with a reduction of only approx. -7%.

The EDT shows similar relative changes due to the variations in ceiling geometry compared to T_{20}. From the initial state, where $EDT_{\text{flat}} = 1.88\,\text{s}$, the deviations in the maximum ceiling state are within $\Delta EDT_{\text{max}} \in [0, -17]\%$. An exception to the changes that mainly appear to be proportional to the ceiling geometry deformation is the unstructured pyramid shaped ceiling. The majority of its changes occur only in the first half of the deformation series. From then on, the ceiling geometry has almost no influence on the EDT.

3.2. Energy components

The total sound strength G is slightly changed when varying the height of the ceiling geometry, as can be seen in Fig. 3. Stepped ceiling surfaces lead to lower values of G, while the maximum change relative to the flat ceiling state where $G_{\text{flat}} = 5.5\,\text{dB}$ is $\Delta G_{\text{stepped,pyramid}} = -0.54\,\text{dB}$. Unstructured surfaces lead to a slight increase in G over the span of changing the ceiling height. The maximum deviation from the flat ceiling state is $\Delta G_{\text{pyramid}} = 0.32\,\text{dB}$. By looking at G_{early} and G_{late}, a large proportion of the changes in G can be attributed to the late sound energies from 80 ms and beyond. Relative changes from the flat ceiling state, where $G_{\text{late,flat}} = 2.62\,\text{dB}$, are within a range of $\Delta G_{\text{late}} \in [-0.92,\ 0.54]\,\text{dB}$.

Early energy components deviate slightly, but are not proportional to the ceiling geometry height. From the flat ceiling state, where $G_{\text{early,flat}} = 2.33\,\text{dB}$, the maximum deviations are within the range of $\Delta G_{\text{early}} \in [-0.17,\ 0.34]\,\text{dB}$.

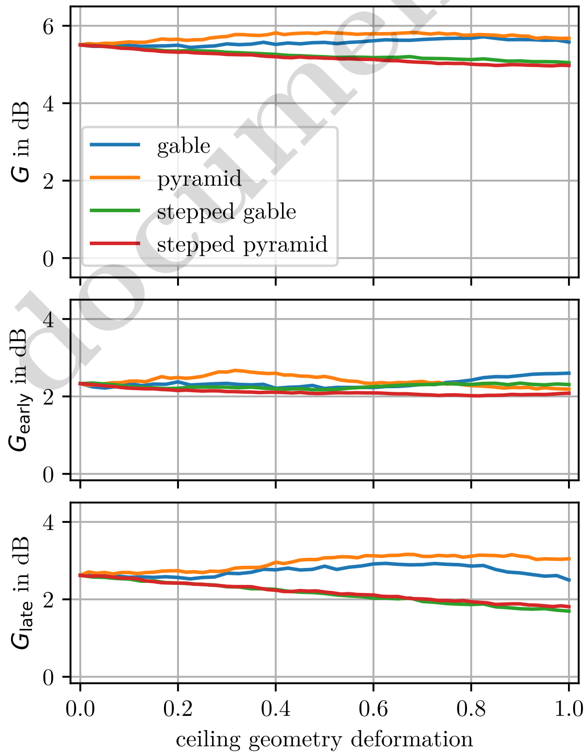

Figure 3: Sound strength G as well as the early and late sound strength G_{early} and G_{late} during the incremental deformation of four ceiling geometries from flat or horizontal to their maximum ceiling shape.

3.2.1. Temporal changes in sound energy

Changes in G_{late} of, for example, the unstructured pyramid-shaped ceiling variant can be seen by inspecting $G_{\text{late}}(\tau = 80\,\text{ms})$ in Fig. 4. The effect of a rising $G_{\text{late}}(\tau)$ when the deformation of the ceiling increases can be seen in the first 100 ms. After around 150 ms the effect inverts, where late energy parts decrease with increasing ceiling height. This results in a highly non-linear energy decay behaviour caused by non-flat ceilings. This pivoting behaviour in the first 10 dB of $G_{\text{late}}(\tau)$ can be seen as the cause of the changes in the EDT.

In Fig. 5, the decays of sound energy $G_{\mathrm{late}}(\tau)$ from the simulated concert hall with stepped pyramid ceilings are shown. Again, as can be seen in the reverberation parameters and the sound strength components, nearly all changes disappear when structuring the ceiling surfaces in a stepped pattern. Only the decrease in total sound strength remains visible as an overall lowering of $G_{\mathrm{late}}(\tau)$ while the slope of the decay curve is nearly unchanged.

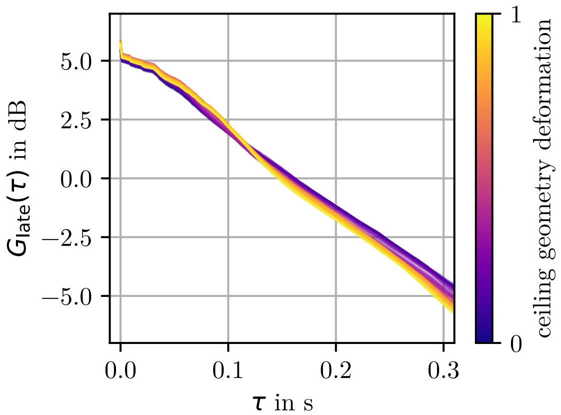

Figure 4: $G_{\mathrm{late}}(\tau)$ and thus the normalized energy decay curve during the incremental deformation of the pyramid shaped ceiling with an unstructured surface from flat or horizontal to its maximum ceiling shape.

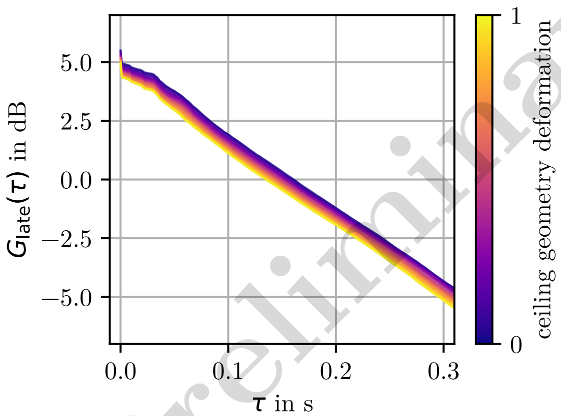

Figure 5: $G_{\mathrm{late}}(\tau)$ and thus the normalized energy decay curve during the incremental deformation of the pyramid shaped ceiling with a stepped surface from flat or horizontal to its maximum ceiling shape.

3.3. Spatial sound incidences

The results of the spatial parameters state only little changes in the parameters associated with ASW. The early lateral energy remains nearly constant across all ceiling states and variants starting from $J_{\mathrm{LF,flat}} = 0.3$. The unstructured gable ceiling variant, as an exception, exceeds the JND of ISO 3382-1 [6] in deformation states, where the total ceiling height accounts for more than 67% of the total room height. Equal behaviour to J_{LF} can be seen in the ASW-linked time period from Green et al. [7], here represented by $G_{\mathrm{lateral,5\,ms-60\,ms}}$. Parameters associated with LEV present more substantial changes. The relative late lateral sound level L_{J} is reduced by variants of stepped ceilings from the initial state where $L_{\mathrm{J,flat}} = -1.63\,\mathrm{dB}$ by an average of $\Delta L_{\mathrm{J,stepped}} = -0.95\,\mathrm{dB}$ in its maximum states. Unstructured ceiling variants differ from this behaviour by rising if the ceiling structure height is more than approx. 27% of the total room height. From the directional analysis of the time periods from Green et al. [7], these changes can be attributed to direction independent sound incidences in the time interval of 80 ms to 150 ms. The maximum differences between unstructured and stepped ceiling variants in the three directional analysis range from 0.7 dB (front/back) to 1.2 dB (lateral).

4. Discussion

The results state that the shape of the ceiling can heavily influence the reverberation time, as well as the early decay time, depending on its surface structure. Inclined unstructured ceiling surfaces lead to a strong decrease in reverberation time, whereas usual measures of sound energy components, such as early, late, and total sound strength, tend to rise slightly. By further inspecting the slope of the energy decay $G_{\mathrm{late}}(\tau)$, this observation can be explained. The higher the ceiling structure, the more nonlinear the sound decay behaviour becomes. Early sound energies of the impulse response until around $80-100$ ms decay in a nearly unchanged way but rise in total with increased ceiling deformation. Therefore, the majority of early reflection patterns are mostly preserved. They are composed of all first reflections, which do not interact with the ceiling surfaces. The subsequent components from $80-100$ ms to 150 ms mark a pivot point where the most relevant changes occur in the contribution of sound energy. This is due to the delay of energies that interact with the ceiling, which gather until they arrive as a cluster after approximately $80-100$ ms. This point in time is likely to vary depending on the room volume and especially the total room height as both aspects change the time of arrival of 1$^{\mathrm{st}}$ to 3$^{\mathrm{rd}}$ order ceiling reflections. By this, indications from common extended sound strength parameters such as G_{early} and G_{late} may be misleading due to different energy contributions from the ceiling in the time region of around 80 ms after direct sound. Due to the strong energy contribution in the first part of the impulse response, latter energies after around 150 ms are attenuated more and more pronounced. In total, this creates a faster decay of sound energy, and thus a reduction in T and EDT.
However, the height of the stepped ceiling shapes only slightly influences T, the EDT, and sound energy components such as G, G_{early}, and G_{late}, as their changes are small compared to other variants of ceiling surfaces. These variations can be attributed to the

increase in total surface area. Interestingly, the slope of the sound energy decay $G_{\mathrm{late}}(\tau)$ remains nearly identical and linear. Consequently, energies are contributed in a similar way in terms of their temporal structure, and the majority of reflection patterns are preserved. Reflections from interactions with the ceiling are spread in time, but are distributed more evenly compared to the unstructured ceiling variants. Losses in sound energy created by an additional surface area in the upper hall section contribute more gradually over the span of the late decay.

The origin of the changes in T, the EDT, and the sound strengths can be estimated by correcting the simulated parameters by the theoretical influence of the change in the surface area of the concert hall. This is done using Sabine's statistical reverberation theory. The corrected values therefore represent changes where only geometrical factors influence the results. Considering the correction, the effect of raked stepped surfaces is nearly mitigated and the changes due to unstructured, raked ceilings are amplified. It can be concluded that the majority of the effects in the simulation results from unstructured ceiling variants are due to the sole change in ceiling geometry.

According to statistical reverberation theory, a linear decay of sound energy is expected when the sound field is sufficiently diffuse. Therefore, the nonlinear energy decay created by raked unstructured ceilings suggests a less diffuse sound field. The audience, as the main absorption area, contributes disproportionally to the loss of sound energy. Stepped ceiling surfaces, on the other hand, preserve the state of diffusivity. Additionally, vertical or parallel surfaces in the upper hall are beneficial for preservation of energy and create a certain "reverberation reservoir". The effect caused by structuring the ceiling in a stepped manner cannot be replicated by increasing the scattering properties of the unstructured ceiling surfaces.

Perceptual impacts on the spatial impression can be concluded by considering changes in the spatial distribution of energy incidences. In general, changes in parameters that are predictors of LEV and ASW can be observed but are either below their JND or take up only a small portion of common values specified in the literature. Both parameters consider lateral sound energy contributions, but variations could be observed from all directions. The only perceptually relevant difference caused by the change in ceiling geometry is observed in the EDT and thus the perceived (running) reverberation. If the height of the unstructured ceiling structures exceeds $28.6\% - 33.9\%$ of the total ceiling height, the JND of $\Delta EDT = 5\%$ specified in ISO 3382-1 [6] is passed. Thus, flat and raked ceilings are likely to be perceived differently in terms of reverberation. Nevertheless, further quantification of the effect on SI requires a listening test.

5. Conclusion

A series of simulations has been conducted, in which the total height, shape, and surface properties of ceiling geometries have been varied. The results state that the shape of the ceiling has a decisive influence on the reverberation in concert halls. When the total geometry is altered from horizontal or flat and thus its surfaces are tilted, the reverberation time and the early decay time drop. Simultaneously, the slope of the sound energy decay behaves more non-linear. Both effects can be counteracted by structuring the ceiling surfaces in a stepped manner, where parallel surfaces can preserve sound energy.

In addition to the EDT, which is modified by the inclined ceiling beyond its JND, when the total ceiling shape accounts for more than approx. 30% of the total room height, a relevant perceptual effect could not be predicted by parameters estimating SI. Further statements about the perceptual effect of ceiling shapes require a listening test.

Further details of this research are presented in [8].

References

[1] L. L. Beranek, *Concert Halls and Opera Houses: Music, Acoustics, and Architecture*, 2nd ed. Springer New York, NY, Apr. 2004, ISBN: 978-1-4419-3038-5.

[2] A. H. Marshall and M. Barron, "Spatial responsiveness in concert halls and the origins of spatial impression," *Applied Acoustics*, vol. 62, no. 2, pp. 91–108, Feb. 2001, ISSN: 0003-682X. DOI: 10.1016/S0003-682X(00)00050-5.

[3] T. Hidaka, L. L. Beranek, S. Masuda, N. Nishihara, and T. Okano, "Acoustical design of the Tokyo Opera City (TOC) concert hall, Japan," *The Journal of the Acoustical Society of America*, vol. 107, no. 1, pp. 340–354, Jan. 2000, ISSN: 0001-4966. DOI: 10.1121/1.428308.

[4] T. Jüterbock, U. Finnendahl, M. Worchel, D. Wujecki, M. Alexa, and S. Weinzierl, "misuka: An open-source differentiable room acoustic renderer," *Proc. of Meetings on Acoustics*, vol. 58, no. 1, 022004:1–022004:13, Jan. 2026, ISSN: 1939-800X. DOI: 10.1121/2.0002193.

[5] *ISO 9613-1:1993(E), Acoustics - Attenuation of sound during propagation outdoors - Part 1: Calculation of the absorption of sound by the atmosphere*, Jun. 1993.

[6] *ISO 3382-1:2009-10, Acoustics - Measurement of room acoustic parameters - Part 1: Performance spaces*, Jun. 2009.

[7] E. Green, E. Kahle, V. Berrier, and E. Carayol, "Beyond 80ms: The Subjective Effects of Sound Energy Arriving Shortly After the "Early" Sound Period," in *Proc. of the International Symp. on Room Acoustics*, Amsterdam, Netherlands, 2019, pp. 483–490.

[8] L. Staubach, "The influence of ceiling shape on spatio-temporal sound energy incidences in concert halls," *Technische Universität Berlin*, 2026. DOI: 10.14279/depositonce-26174.